

## Numerical study of composite structures subjected to slamming loads using Smoothed Particle Hydrodynamics (SPH)

Kameswara Sridhar Vepa<sup>1</sup>, Diederik Van Nuffel<sup>1</sup>, Wim Van Paepegem<sup>1</sup>, Joris Degrieck<sup>1</sup>

<sup>1</sup>Department of Materials Science and Engineering, Ghent University, Sint-Pietersnieuwstraat 41, B-9000 Gent, Belgium  
email: KameswaraSridhar.Vepa@Ugent.be, diderik.vannuffel@ugent.be, Wim.VanPaepegem@Ugent.be, Joris.degrieck@Ugent.be

**ABSTRACT:** Since the inception of composite materials in the field of marine applications, there has been an ever increasing demand for more cost efficient, and low weight composite structures. This has led to a drastic reduction in the amount of material used, which rendered these structures deformable especially under severe loading conditions like slamming wave impact. Slamming loads are characterised by large local pressures, which last for very short durations of time and move very fast along the surface of the structure. Deformation of the structure dampens the pressure intensity on the surface of the structure. In this study, the response behaviour of deformable composite structures subjected to slamming loads is studied using the existing numerical methods for Fluid-Structure Interaction (FSI) and free surface flows as slamming loads are generally observed in marine applications. Numerical simulations are done using explicit smoothed particle hydrodynamics (SPH) codes. Results from the numerical models are validated using the experimental rigid body slamming studies that are already existing and the same numerical models are used for studying the behaviour of the deformable composite structures.

**KEY WORDS:** Slamming, Composite structures, Fluid Structure Interaction, free surface flow.

### 1 INTRODUCTION

Wave impact or slamming is one of the critical design criteria for any offshore structure[1-4]. It is characterized by high local peak pressures with very short time durations. Though the local peak pressures last for short durations, they can cause severe damage to the incident structure. Also, composite materials are finding more and more applications in offshore constructions and the study of response behaviour of these composite structures to slamming loads is very critical. In the case of offshore constructions like wave energy convertors, where the surface can be allowed to deform, it is very important to accurately measure the magnitude of the local peak pressures, as it helps in the better understanding of the influence of the slamming loads.

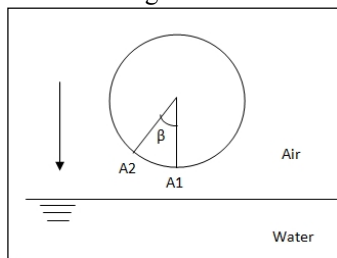


Figure 1 : Cylinder hitting water surface

The shape of the structure that is subjected to slamming is also critical in evaluating its response behaviour. Hence, as a specific test case, a deformable composite 2D cylinder is tested for the slamming loads. Figure 1 shows the water entry configuration of a cylinder. It can be seen in the simulations that the elements that are at the bottom-most point are flat with a dead rise angle of  $\sim 180$  degrees and as we move up the cylinder surface, the angle reduces to 90 degrees.

SPH method is proved to be successful in modelling the free surface flows with good accuracy[5]. SPH method is a mesh free method and has the characteristics of a lagrangian method. This helps in modelling the breaking of interface accurately. Hence it is applied for modelling the free surface impact problem in this case.

### 2 PRINCIPLE USED

Distribution of hydrodynamic pressures is highly localised in space and time. This makes the modelling of slamming wave impact a computationally challenging task. Slamming loads also depend on the shape of the body subjected to slamming[6]. Two cylinders of same dimensions are compared. The first one is a rigid cylinder which is not allowed to deform. The second cylinder is a hollow cylinder made of a composite shell which shows large deformations during impact. The cylinders have a diameter of 0.3 m and a length of 0.4 m. Comparing the impact pressures of both cylinders can result in useful information on the effect of deformability during water impact.

In general, wave slamming is a fluid-structure interaction problem with multi-phase flow field[7]. Hence, numerical modelling of slamming wave impact includes: 1) multiphase modelling of free surface flow subjected to gravity load, 2) Fluid structure interaction between the body and the fluids (air and water), and 3) Contact modelling between the fluids as well as fluid and structure.

Multiphase modelling of free surface flow is done numerically by solving the continuity equation and Navier-Stokes equations with kinematic and dynamic boundary conditions imposed on the flow field. Equation 1 represents the continuity equation where  $V$  is the fluid velocity field. Equation 2 shows the Navier-Stokes equations where  $\rho$  represents density,  $p$  represents pressure and  $v$  represents

viscosity. Kinematic boundary conditions are used to specify the conditions like no-slip and no-flux boundaries. Equation 3 shows no slip boundary condition near the solid boundary which represents finite shear stress. Here,  $U$  is the velocity of the solid boundary. Equation 4 shows the no-flux boundary condition at the solid boundary which represents a continuous flow. Dynamic boundary conditions are used to specify the dynamics of the boundary like the stress continuity. In case of a free surface, pressure outside the fluid is considered constant and is equal to atmospheric pressure. This is shown in equation 5.

$$\nabla \cdot \vec{V} = 0 \tag{1}$$

$$\frac{\partial v}{\partial t} + (\vec{V} \cdot \nabla) \vec{V} = -\frac{1}{\rho} \nabla p + \nu \nabla^2 \vec{V} \tag{2}$$

$$\vec{V} \cdot t = \vec{U} \cdot t \tag{3}$$

$$\vec{V} \cdot \hat{n} = \vec{U} \cdot \hat{n} \tag{4}$$

$$\frac{dp}{dt} = 0 \tag{5}$$

Based on the characteristic fluid velocities, the mach number is much less than unity, and hence the fluids are considered incompressible + inviscid (=ideal). Also, the flow is considered irrotational and the surface tensions are neglected.

### 3 EXPERIMENTAL TEST OBJECTS

#### 3.1 Rigid material

Highly stiff material that does not allow any deformations at tested velocities is used. The inside of the cylinder is made of polyurethane foam with a density of  $100 \text{ kg/m}^3$  to make it rigid and low weight at the same time. To make it as rigid as possible, the foam is covered with a shell of glass fibre reinforced composite material (Refer Figure 2). The shell is composed of two layers of continuous fibres wound around the foam with an angle of  $70^\circ$  with reference to the axis of the cylinder and embedded in an epoxy matrix.

Rigid cylinder tests are done not just for comparison with deformable materials but also for comparison with the existing literature. This helps in understanding the reliability of the code for fluid-structure interactions.

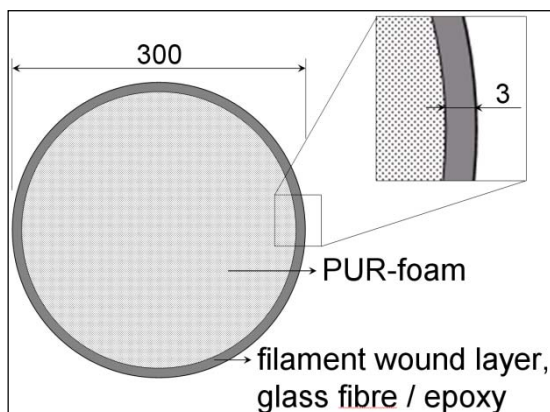


Figure 2 : Rigid Material

#### 3.2 Deformable material

The deformable material is made out of a glass fibre reinforced composite shell of three layers. The first layer is a quasi isotropic chipped glass fibre material embedded in an epoxy matrix. The two next layers are layers of continuous glass fibres wound with an angle of  $70^\circ$  with reference to the axis of the cylinder. The total thickness of the composite shell is about 3 mm (refer Figure 3).

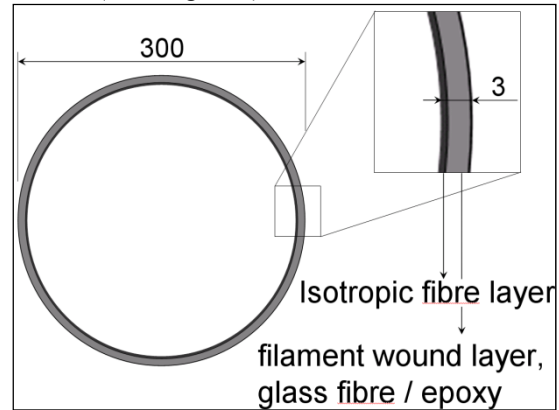


Figure 3 : Composite Material

### 4 EXPERIMENTS AND DISCUSSION

The experimental set-up that is used is for the slamming experiments is shown in Figure 4. In this set-up, it are not the waves which are slammed against the structure, but the structure that is slammed against a free water surface. The set-up consists of a water reservoir which measures  $1.5 \times 1.2 \text{ m}$  and has a water depth of  $0.64 \text{ m}$ . A stepladder which is present adjacent to the water reservoir operates as a lever beam to pull up the test object and drop it from a specified height into the water reservoir. This is realised by means of a rotating shaft, connected to the ladder and to an electric AC-motor which is operated by a programmable motor control unit. The AC motor makes it possible to pull up the ladder automatically without manual operations and to adjust the drop height precisely.



Figure 4 : Experimental Test setup

All experiments are performed with different drop heights upto  $1.2 \text{ m}$  above the water surface. This drop heights result in a maximum measured vertical impact speed  $V_{\text{impact}}$  of about  $4.51 \text{ m/s}$  at the moment of first contact of the cylinder with the water surface as shown in Figure 5. The results of the pressure measurements, for different deadrise angles for  $V_{\text{impact}}$  of  $3.4 \text{ m/s}$ , for the rigid and the deformable cylinder are shown in Figure 6 and Figure 7. The pressure results are represented

with a non-dimensional coefficient, i.e. the pressure coefficient  $C_p$  which is calculated using equation 6 where  $p_{max}$  represents maximum pressure.

$$C_p = \frac{p_{max}}{0.5 \cdot \rho \cdot V^2} \tag{6}$$

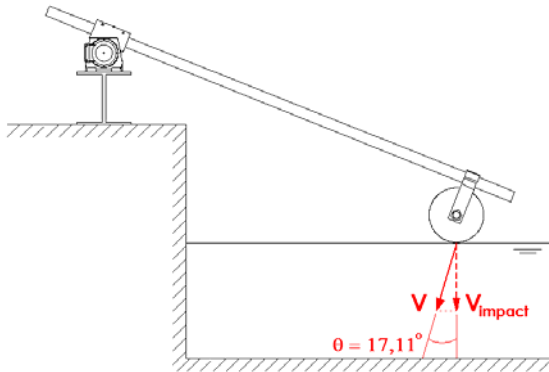


Figure 5 : Angle of impact

For the rigid cylinder for  $V_{impact}$  of 3.4m/s, the experimental results are compared with the experimental results of Lin and Shieh[8] as shown in Figure 6. It can be seen that there is a good correspondence for deadrise angles higher than 10°. For deadrise angles smaller than 10°, the difference is due to the difference in sampling rate of the data acquisition system during the pressure measurements. In Lin and Shieh[8], a sampling rate of 25 kHz is used, while it was 100 MHz during the experiments of this paper. The lower pressure values for small deadrise angles in the experiments of Lin and Shieh[8] are due to the fact that for small deadrise angles, the pressure peaks at a certain point are that short in time that they occur between two samples taken by the data acquisition system corresponding to 200 kHz.

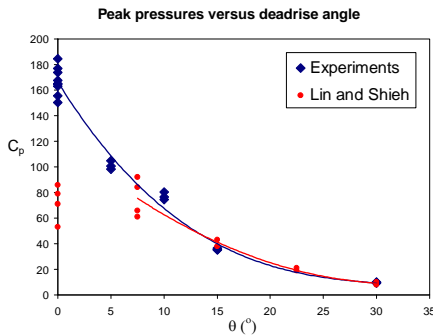


Figure 6 : Peak pressures for rigid cylinder

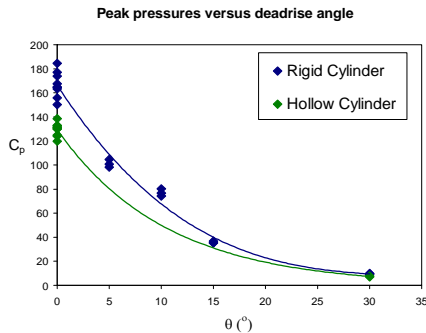


Figure 7 : Coefficient of pressure for rigid and deformable cylinder

## 5 SIMULATIONS AND DISCUSSION

To capture the pressure profiles accurately along the surface of the cylinder, two methodologies have been used here : 1) modelling both the fluid as well as structure using SPH particles and 2) Coupling the finite element mesh of the structure with fluid SPH particles. Later, these results are compared with the results from the experiments.

### 5.1 Pure SPH simulations

Bucket sorting method is used in finding the neighbours for a particle. Artificial viscosity is used to take care of the shocks. Time integration is done using the classical first order method. Though it increases the number of particles, a regular SPH mesh is used to reduce the inter-particle discrepancies.

The SPH method has proven to be successful in modelling the free surface flows with good accuracy[9]. SPH has the characteristics of a lagrangian method. This helps in modelling the breaking of interface accurately. Hence it is applied for modelling the free surface impact problems as in this case[10]. The basic equation solved is the Navier-Stokes equation as given by equation 2. An interpolation scheme as shown in equation 7 can be used for calculating the lagrangian derivatives at each point in the domain D. Finally, numerical integration is done using a quadrature formula like the one shown in equation 8 at every integration point i. Instability is one drawback of this method due to the explicit time integration scheme. To overcome this, an artificial viscosity term is added to the momentum equation. This could be a drawback if used in low-dynamics flows, but for shocks and explosions where, good conservation of energy is not needed, this still gives good results.

$$f(\vec{r}) \approx \int_D f(\vec{x})W(\vec{r} - \vec{x},h)d\vec{x} \tag{7}$$

$$\int_D g(\vec{x})d\vec{x} \approx \sum_i g_i w_i \tag{8}$$

Figure 8 shows the schematic model used for the simulation. Here we can clearly see that air is not modelled and water with free surface boundary condition is used. Hence the SPH simulation is reduced to a single phase simulation. Figure 9 shows the corresponding SPH model. In order to make the cylinder rigid, a cylinder with very high stiffness value is used as it is not possible to model cylinder to be completely rigid using the SPH equations.

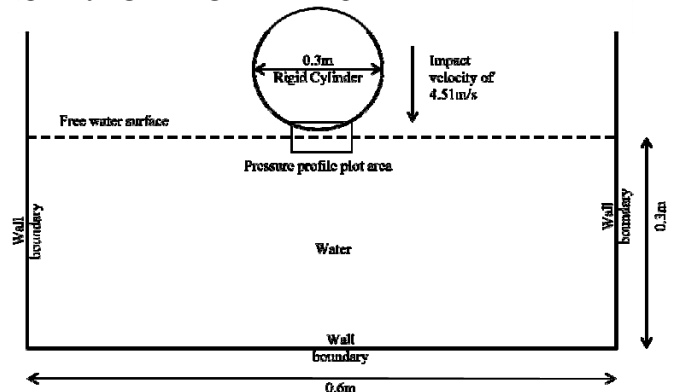


Figure 8: Schematic model

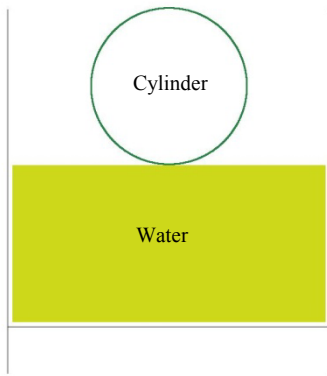


Figure 9 : SPH model used for pure SPH simulations

In Figure 10, the pressure peaks at the bottom of the cylinder are plotted against time. It can be seen that observed pressures are very high and are about 67 bar which do not match with the experimental values. Two points to be noted here are: 1) Calculated pressures are very high, and 2) It is not possible to model the composite material using the SPH particles with the commercial code. Hence a coupling with the Finite element solver is used to calculate the slamming impact pressures, which is discussed in section 5.2.

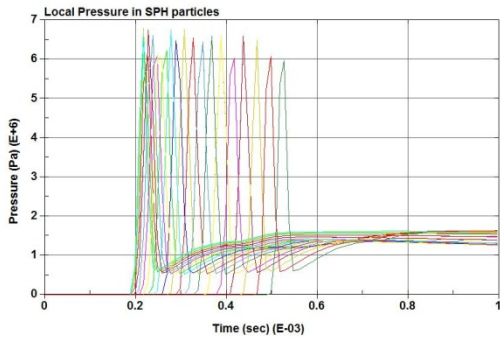


Figure 10: Pressure profiles at the bottom of the cylinder

5.2 Coupled SPH-FEM simulations (rigid cylinder)

Since SPH is a particle based lagrangian method, the water surface is tracked based on the particle position. The smallest particle size of 1mm is used and also the velocity of the cylinder in the numerical simulations is compared with that of the experimental data. A total of 270000 particles are used for the simulation with the particle size of 1 mm. Shell elements are used for modelling the rigid and composite cylinders. Shell elements of uniform size (approximately 6 mm) are used for representing the cylinder.

The density of the water is taken as 1000 kg/m<sup>3</sup> and is treated as compressible fluid. Based on the smallest particle size, the time step size is decided using the dimensionless Courant number, which is calculated based on the velocity of the cylinder. Equation 9 is used to calculate the time step of the simulation.

$$\frac{\vec{v} \cdot \Delta t}{\Delta x} \leq C_{CFL} \tag{9}$$

Figure 11 shows the simulation model with the pressure distribution in the water domain.

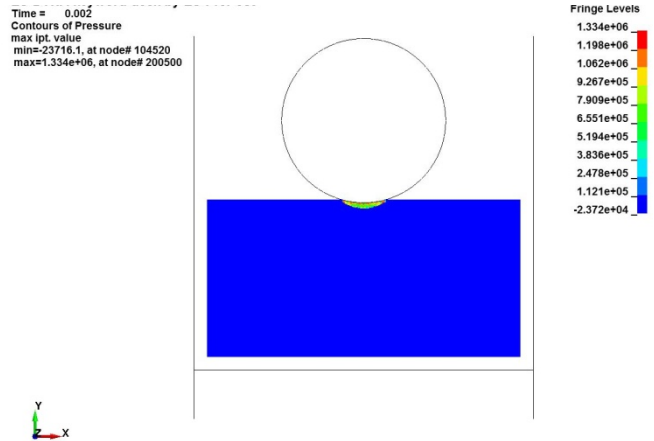


Figure 11: Coupled SPH-FEM simulation model with pressure profiles

Figure 12 shows the pressure contours at the bottom of the cylinder. It is observed the pressures occur at the bottom most point of the cylinder or the first point of contact on the water surface.

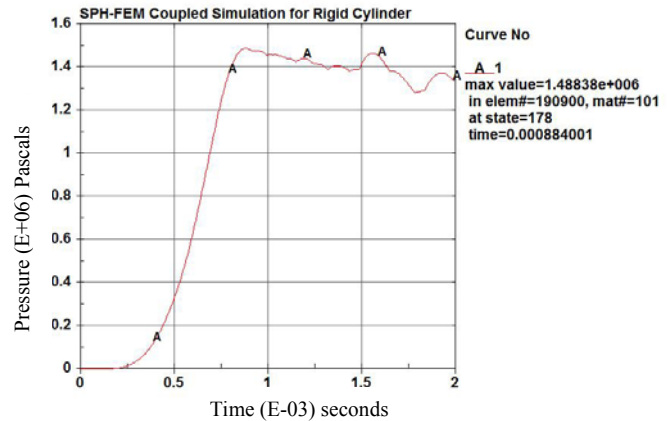


Figure 12: Peak pressure for the rigid cylinder

Peak pressure of 14.8 bar observed in the coupled simulation is in close agreement with that of the experimental value. Experimental observations for the same impact velocity show a peak pressure of 14.7 bar. Slight variation the calculated pressure can be attributed to the experimental errors and the modelling simplifications like ignoring the presence of air above the water surface.

Figure 13 shows the pressures curves of the particles as we move away from the bottom most point of the cylinder. It can be observed that the peak pressure moves along the surface of the cylinder and slowly decreases as it progresses.

5.3 Coupled SPH-FEM simulations (composite cylinder)

Simulation model for the composite cylinder is same as the one used for the rigid cylinder except for the material model used for the cylinder. Figure 14 shows the pressure profile for the SPH particle that first comes in contact with the cylinder.



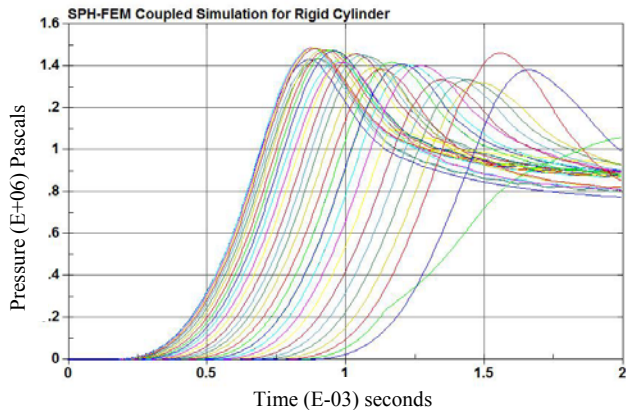


Figure 13: Pressure profiles at the bottom of rigid cylinder

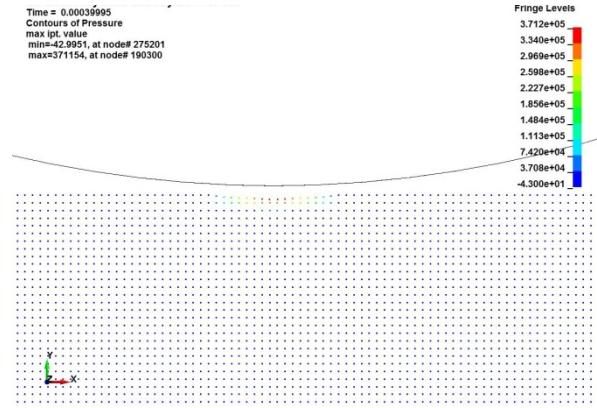


Figure 16: SPH particle distribution and the composite cylinder hitting the water surface

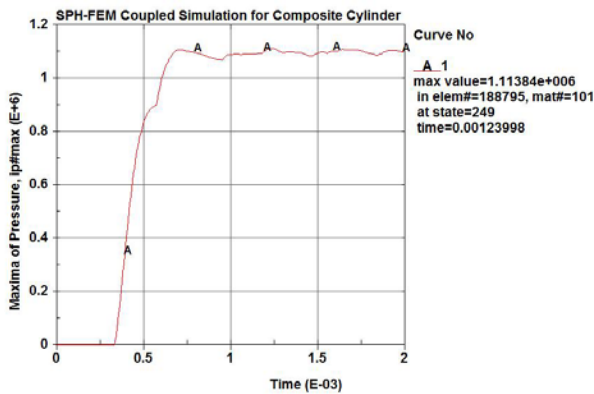


Figure 14: Peak pressure observed at the bottom of the composite cylinder

Figure 15 shows the peak pressure curve as it moves along the surface of the cylinder.

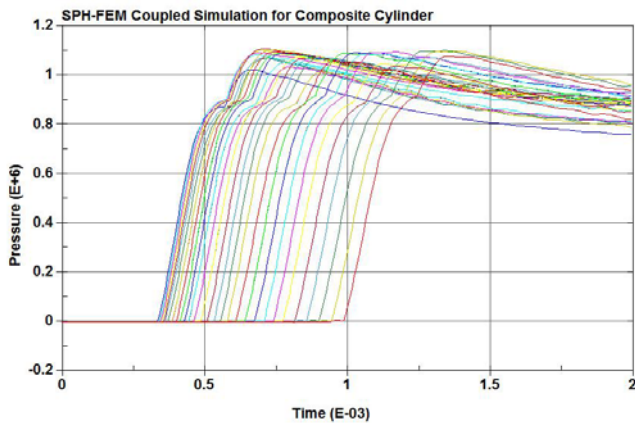


Figure 15 : Pressure profiles at the bottom of composite cylinder

Figure 16 shows the SPH particle distribution and peak pressure observed at the first point of contact of the cylinder.

Table 1 shows the peak pressure comparison for the rigid cylinder simulations done using pure SPH methods and the SPH-FEM coupling.

Table 1: Comparison of peak pressures for rigid cylinder

| Impact velocity of 4.51 m/s | Peak pressure observed in rigid cylinder |
|-----------------------------|--|
| Pure SPH                    | 67 bar                                   |
| SPH_FEM coupling            | 14.7 bar                                 |
| Experimental                | 14.8 bar                                 |

Table 2 shows the peak pressure comparison for the composite cylinder simulations done using the SPH-FEM coupling and the experimental data.

Table 2 : Comparison of peak pressures for rigid cylinder

| Impact velocity of 4.51 m/s | Peak pressure observed in rigid cylinder |
|-----------------------------|--|
| SPH_FEM coupling            | 11.13 bar                                |
| Experimental                | 11.69 bar                                |

Table 3 shows the comparison of peak pressures for composite cylinder using SPH-FEM coupling.

Table 3 : Comparison of peak pressures for composite cylinder

| Impact velocity of 4.51 m/s | Peak pressure observed |
|-----------------------------|------------------------|
| Rigid cylinder              | 14.7 bar               |
| Composite cylinder          | 11.13 bar              |

From the experiments, it is observed that the decrease in peak pressure when deformations are allowed in the cylinder is 21.1% whereas the decrease in peak pressure from numerical simulations is 24.28% for an impact velocity of 4.51m/s. Keeping the scatter in view for the experimental

data, in can be concluded that the numerical simulations are in good agreement with the experimental data.

#### 5.4 Computational time

A bucket sorting method is used in finding the neighbours for Table 4 shows the calculation times for rigid cylinder simulations in pure SPH and coupled SPH-FEM simulations. It can be observed that the calculation times are much higher for pure SPH simulations. Problem time for this particular modes is 1e-2 seconds.

Table 4 : CPU times for rigid cylinder simulations using pure SPH and coupled SPH-FEM methods.

| Impact velocity of 4.51 m/s | CPU time in seconds |
|-----------------------------|---------------------|
| Pure SPH method             | 33367               |
| Coupled SPH-FEM method      | 18284               |

This shows that the pure SPH is computationally costly and also accuracy in this case is not observed but in the case of coupled method, CPU time required for the solver is low as well the accuracy of the results is also observed.

## 6 CONCLUSIONS

Using the Smoothed particle hydrodynamics methods, two cases are studied in this paper. Firstly, choice of the solver for simulating a wave slamming problem. Secondly, effect of deformability on the incident local peak pressures during the slamming experiments.

From the observations for the choice of the solver, it is clear that pure SPH method is computationally costly as compared to the coupled SPH-FEM solver and the quality of the results is also in good agreement with the experimental results.

Coming to the effect of deformability, it is clear that the deformability decreases the magnitude of the incident peak pressures coming on to the cylinder due to the wave slamming. Also, there is percentage decrease in the peak pressure is 24.28% which shows that the allowance for deformation in the cylinder helps in reducing the incident wave loads due to slamming. But, it is also important to check for the damage in the structure as well as the sustainability of the structure when subjected to regular slamming loads. This has to be studied further.

Advantages of both particle based methods as well as the mesh based methods are utilized in the coupled SPH-FEM simulation.

## ACKNOWLEDGMENTS

The authors are highly indebted to the university research fund FWO for sponsoring this research.

## REFERENCES

[1] Downs-Honey, R., S. Edinger, and M. Battley, *Slam testing of sandwich panels*. *Sampe Journal*, 2006. **42**(4): p. 47-55.  
 [2] Sebastiani, L., et al., *A theoretical / experimental investigation of the slamming pressures on fast monohull vessels*. *Fast-2001*, 2001.  
 [3] Faltinsen, O.M., M. Landrini, and M. Greco, *Slamming in marine applications*. *Journal of Engineering Mathematics*, 2004. **48**(3): p. 187-217.

[4] Wienke, J. and H. Oumeraci, *Breaking wave impact force on a vertical and inclined slender pile--theoretical and large-scale model investigations*. *Coastal Engineering*, 2005. **52**(5): p. 435-462.  
 [5] Monaghan, J.J., *Smoothed particle hydrodynamics*. *Reports on Progress in Physics*, 2005. **68**(8): p. 1703-1759.  
 [6] Mei, X., Y. Liu, and K.P. Yue Dick, *On the water impact of general two-dimensional sections*. *Applied Ocean Research*, 1999. **21**(1): p. 1-15.  
 [7] Agamloh, E.B., A.K. Wallace, and A. von Jouanne, *Application of fluid-structure interaction simulation of an ocean wave energy extraction device*. *Renewable Energy*, 2008. **33**(4): p. 748-757.  
 [8] Lin, M.-C. and L.-D. Shieh, *Flow visualization and pressure characteristics of a cylinder for water impact*. *Applied Ocean Research*, 1997. **19**(2): p. 101-112.  
 [9] Oger, G., et al., *Two-dimensional SPH simulations of wedge water entries*. *Journal of Computational Physics*, 2006. **213**(2): p. 803-822.  
 [10] Fang, J., et al., *Improved SPH methods for simulating free surface flows of viscous fluids*. *Applied Numerical Mathematics*, 2009. **59**(2): p. 251-271.